Early events in the folding of four-helix-bundle heme proteins

Jasmin Faraone-Mennella, Harry B. Gray†, and Jay R. Winkler†

Beckman Institute, California Institute of Technology, Pasadena, CA 91125

Contributed by Harry B. Gray, March 21, 2005

Topologically homologous four-helix-bundle heme proteins exhibit striking diversity in their refolding kinetics. Cytochrome b_{562} has been reported to fold on a submillisecond time scale, whereas cytochrome *c′* refolding requires 10 s or more to complete. Heme dissociation in cytochrome b_{562} interferes with studies of folding kinetics, so a variant of cytochrome b_{562} (cytochrome *c*-b_{562}) with a covalent *c*-type linkage to the heme has been expressed in *Escherichia coli*. Early events in the electron transfer-triggered folding of Fe^{II}-cytochrome *c*-b_{562}, along with those of Fe^{II}-cytochrome c_{556}, have been examined by using time-resolved absorption spectroscopy. Coordination of S(Met) to Fe^{II} occurs within 10 μs after reduction of the denatured Fe^{III}-cytochromes, and shortly thereafter (100 μs) the heme spectra are indistinguishable from those of the folded proteins. Under denaturing conditions, carbon monoxide binds to the Fe^{II}-hemes in $\approx$15 ms. By contrast, CO binding cannot compete with refolding in the Fe^{II}-cytochromes, thereby confirming that the polypeptide encapsulates the heme in <10 ms. We suggest that Fe-S(Met) ligation facilitates refolding in these four-helix-bundle heme proteins by reducing the conformational freedom of the polypeptide chain.

cytochrome | electron transfer | protein folding

Whether topologically similar proteins necessarily have similar folding pathways is an open question (1). With the increasing number of structures available, it has become clear that polypeptide sequences with little or no homology can assume nearly identical three-dimensional backbone architectures. Theoretical models suggest (2–4), and most experimental studies confirm (5–8), that a helical bundle is a fast folding structural motif. The presence of heme cofactors, however, can introduce new features into the helical bundle energy landscape that can greatly alter refolding pathways.

We have reported previously on the folding kinetics of two four-helix-bundle heme proteins, cytochrome b_{562} (cyt b_{562}) and cytochrome *c′* (cyt *c′*). Although the two cytochromes have nearly identical three-dimensional structures (3.4-Å rms deviation of backbone atoms), they have very low sequence identity (15%) and exhibit quite disparate folding kinetics (9–11). Fe^{II}-cyt b_{562} folds in less than a millisecond, whereas Fe^{II}-cyt *c′* folding is quite heterogeneous, spanning time scales from milliseconds to seconds. Clearly, topology alone does not dictate these refolding rates.

The folding of cyt b_{562} is complicated by heme dissociation from the polypeptide, limiting the refolding yield (11). We suggested that heme dissociation could be responsible for the fast folding observed in cyt b_{562} by selecting against slower-folding populations in the unfolded ensemble. Indeed, a recent investigation of cyt b_{562} suggests that the heme in the denatured protein is bound to a native-like polypeptide conformation that is predisposed to fold rapidly (12).

To circumvent complications arising from heme dissociation, we have engineered a variant of *E. coli* cyt b_{562} (cyt *c*-b_{562}) in which two thioether linkages bind the porphyrin to the polypeptide chain in the fashion of a *c*-type cytochrome (13–15). We also have investigated cytochrome c_{556} from *Rhodopseudomonas palustris* (16), a protein with the same four-helix-bundle fold as cyt b_{562} and cyt *c′* (backbone atom rms deviations vs. cyt b_{562}, 3.3 Å; vs. cyt *c′*, 1.5 Å) (17–20) but with low sequence identity (cyt b_{562}, 21%; cyt *c′*, 34%). Here, we report early events in folding the Fe^{II} forms of *c*-b_{562} and c_{556}.

Materials and Methods

Guanidine hydrochloride (GuHCl, Sigma, ultrapure grade), tris(2,2′-bipyridine)ruthenium(II) chloride ($[Ru(bpy)_3]Cl_2$, Strem), and NADH (Sigma) were used as received.

R. palustris cyt c_{556} was expressed and purified by published procedures with minor modifications (16). The N-terminal glutamine was fully cyclized by heating the protein at 50°C for 5 h in 0.5 M KH_2PO_4 (21). *E. coli* cyt *c*-b_{562} was expressed by cotransforming the construct pETcb562 (unpublished procedure) with pEC86 (22) into *E. coli* strain BL21 (DE3). Cyt *c*-b_{562} was purified by ion exchange chromatography on CM Sepharose Fast Flow and followed by a second purification step on a Mono S column (FPLC, Amersham Pharmacia). Proteins were judged to be pure by SDS/PAGE (PhastSystem, Amersham Pharmacia) and electrospray ionization–MS analysis (Caltech Protein/Peptide Microanalytical Laboratory).

Circular dichroism (CD) spectra were recorded by using an Aviv 62ADS spectropolarimeter; Trp fluorescence spectra were recorded on a Jobin Yvon SPEX Fluorolog-3 spectrofluorimeter (λ_{ex} = 290 nm; λ_{em} = 300–500 nm). Steady-state absorption spectra were recorded on a Hewlett–Packard HP-8453 or HP-8452 diode array spectrometer. Protein (cyt *c*-b_{562}) concentrations were determined by using the extinction coefficients reported for cyt b_{562} (23, 24).

Transient absorption kinetics measurements were made as described in refs. 11 and 25. Folding measurements were performed with solutions buffered to pH 7 with cyt c_{556} and pH 5 with *c*-b_{562} to inhibit misligation of His-63. Samples for folding kinetics measurements [cyt c_{556} or *c*-b_{562} (100 μM); $Ru(bpy)_3^{2+}$ (50–150 μM) or NADH ($\approx$200 μM); GuHCl (1–6 M)] were sealed in 1-mm cuvettes and deoxygenated by repeated evacuation/Ar or CO backfill cycles. GuHCl concentrations were determined after laser experiments from refractive index measurements (Abbe-3L refractometer, Milton Ray, Rochester, NY) (26).

Results and Discussion

Equilibrium Unfolding. Cyt c_{556} and *c*-b_{562} are soluble proteins (molecular masses of 14.7 and 12.3 kDa, respectively). Each folded structure contains four antiparallel α-helices in a left-handed bundle with a heme group located in a hydrophobic pocket near the C and N termini; the porphyrin is covalently bound to the polypeptide chain through thioether linkages with two C-terminal cysteine residues, and the iron center is axially ligated by Met-12 and His-121 (cyt c_{556}) or Met-7 and His-102 (cyt *c*-b_{562}) (18). GuHCl titrations, monitored by absorbance, CD, and tryptophan fluorescence spectra, reveal cooperative

BIOPHYSICS

Abbreviation: cyt, cytochrome.

†To whom correspondence may be addressed at: Beckman Institute, California Institute of Technology, MC 139-74, Pasadena, CA 91125-7400. E-mail: hbgray@caltech.edu or winklerj@caltech.edu.

© 2005 by The National Academy of Sciences of the USA

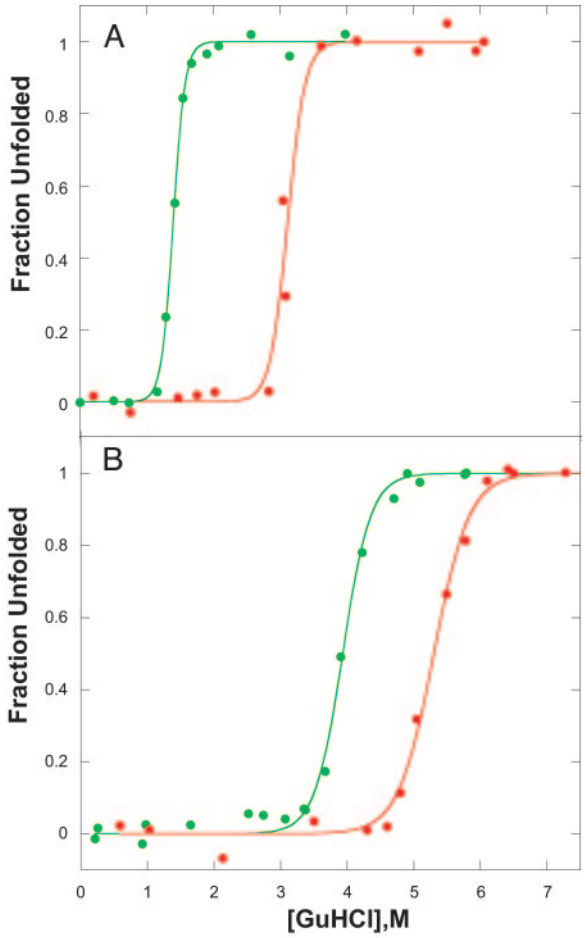

Fig. 1. Denaturant-induced unfolding of Fe^{III} (green) and Fe^{II} (red) c_{556} (*A*) and *c*-b_{562} (*B*). Data points are from CD measurements; data from with heme absorption and Trp fluorescence are virtually the same.

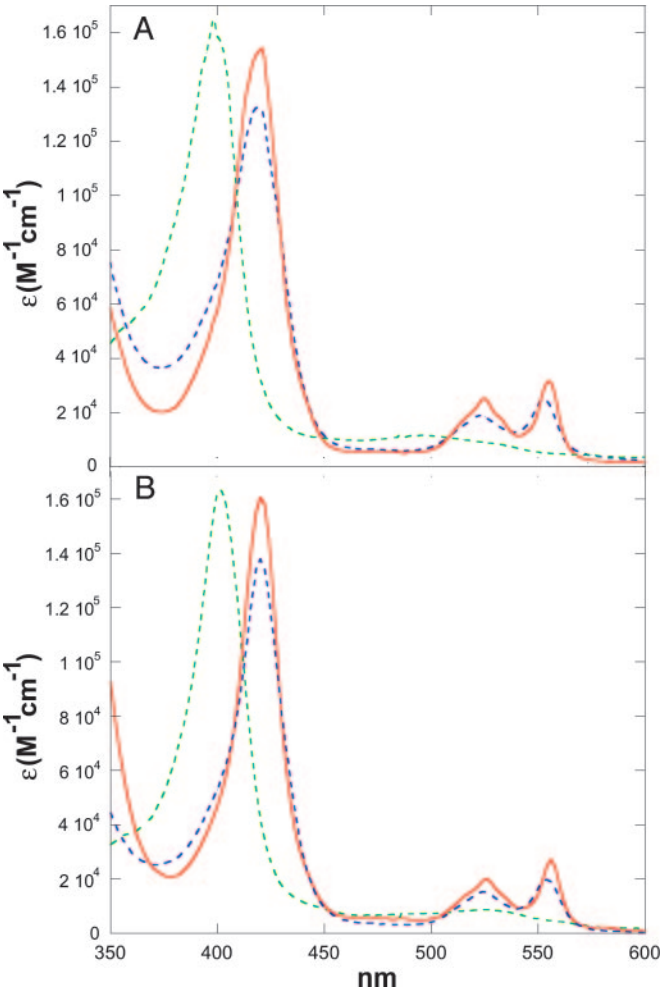

Fig. 2. Absorption spectra of unfolded Fe^{III} (green dashed line), folded Fe^{II} (red dashed line), and unfolded Fe^{II} (blue dashed line) cyt c_{556} (*A*) and cyt *c*-b_{562} (*B*).

unfolding transitions (Fig. 1), and, as expected on the basis of their high reduction potentials, the Fe^{III} forms are less stable than the Fe^{II} proteins (27, 28). It is interesting to note that the introduction of two thioether linkages to the heme in cyt *c*-b_{562} leads to a substantial stabilization of the folded protein (the denaturation midpoint, $[GuHCl]_{1/2}$, increases by ≈2 M).

The absorption spectra of native and denatured $Fe^{III/II}$-cyt c_{556} and $Fe^{III/II}$-cyt *c*-b_{562} (pH 5) are shown in Fig. 2. In both Fe^{III} and Fe^{II} oxidation states, the heme becomes exposed to the solvent upon unfolding, leading to distinct shifts in absorption spectra, including variations in extinction coefficients, which can be exploited to monitor folding kinetics. The blue shift in the Soret absorption upon denaturation of each Fe^{III} protein indicates that the heme has undergone a low- to high-spin transition, likely the result of replacement of the axial methionine ligand with a water molecule. In denatured Fe^{II} forms, however, both Soret and Q-band absorptions suggest that the heme remains low-spin. In contrast to the behavior of unfolded cytochrome *c*, it is not likely that nonnative His coordination accounts for the low-spin hemes in denatured Fe^{II}-cyt c_{556} and Fe^{II}-cyt *c*-b_{562}. Cyt c_{556} has no available His residues, and denaturation of Fe^{II}-cyt *c*-b_{562} was performed at pH 5 to inhibit His-63 misligation. As was suggested for unfolded Fe^{II}-cyt *c*′, methionine residues apparently compete for the sixth Fe^{II} coordination site in the unfolded proteins. In Fe^{II}-cyt *c*-b_{562}, both Met-7 and Met-58 are likely to be involved; Met-12, Met-19, and Met-20, and possibly Met-110, are the candidates in Fe^{II}-cyt c_{556}. Analogous behavior was found in denatured *R. palustris* Fe^{II}-cyt *c*′ where Met-15 and Met-25 are potential ligands (9, 10). Although the absorption spectra of denatured Fe^{II}-cyt c_{556} and Fe^{II}-cyt *c*-b_{562} resemble those of the folded proteins, CD spectra clearly indicate that the native helical secondary structures are substantially disrupted (12).

Electron Transfer-Triggered Refolding. At suitable denaturant concentrations (cyt c_{556}, 1.5–2.5 M; cyt *c*-b_{562} 3.8–4.8 M), electron injection into the denatured Fe^{III} protein will initiate folding of the Fe^{II} form (27). In prior work, we have demonstrated that $Ru(bpy)_3^{2+}$ and NADH are useful sensitizers for photochemical triggering of Fe^{II}-cytochrome refolding (27, 29). Electronically excited $Ru(bpy)_3^{2+}$ [$E°(Ru^{3+/*2+}) = -0.85$ V vs. normal hydrogen electrode] injects an electron into the unfolded protein within a few microseconds. Subsequent charge recombination regenerates the initial reagent in a few milliseconds, allowing extensive signal averaging but limiting the observable window for folding to ≈1 ms. Two-photon excitation (355 nm) of NADH produces two reductants (e^-_{aq} and $NAD^{\cdot}$) that irreversibly reduce the heme group in ≈100 μs (≈100 μM protein) (30). Therefore, with NADH it is possible to expand the observation time window to seconds and longer.

We have used both $Ru(bpy)_3^{2+}$ and NADH to trigger Fe^{II}-cyt c_{556} and Fe^{II}-cyt *c*-b_{562} refolding. In experiments with $^*Ru(bpy)_3^{2+}$ as the photoreductant, the observed transient absorption kinetics depend on denaturant concentration. These

data are adequately described by a biexponential function. The faster rate is independent of [GuHCl] and corresponds to decay of $*Ru(bpy)_3^{2+}$ ($k_1 \sim 1.6 \times 10^6\ s^{-1}$) with parallel reduction of the Fe^{III} protein. The rate constant for the slower phase varies with [GuHCl]; this reaction channel represents early events in the folding of the protein around the heme (Fe-cyt c_{556}, $k_2 = 4\times 10^5$ to $8\times 10^5\ s^{-1}$, [GuHCl] = 3–2 M; Fe-cyt c-b_{562}, $k_2 = 5\times 10^5$ to $2\times 10^6\ s^{-1}$, [GuHCl] = 5.5–4.5 M). The transient spectra measured at the end of the slower phase ($t \sim 100\ \mu s$) are consistent with the formation of reduced folded protein.

Biexponential kinetics also are observed when NADH is used as the photoreductant, with rate constants independent of [GuHCl] that are attributable to the reduction of the protein by e^-_{aq} ($4–5 \times 10^4\ s^{-1}$) and NAD$^{\cdot}$ ($9 \times 10^3\ s^{-1}$). The relative signal amplitudes observed after excitation of samples at low and high [GuHCl] (Fe-cyt c_{556}, 1.5 and 4 M; Fe-cyt c-b_{562}, 4 and 7 M) suggest that folded reduced protein is formed 300 μs after excitation (Fig. 3). No additional changes in absorption were detected on time scales as long as several seconds; the formation of folded reduced protein appears to be limited by the rate of reduction by NAD$^{\cdot}$. Moreover, steady-state UV-visible and CD spectra recorded after laser excitation of NADH-containing samples confirm that the photochemically reduced proteins adopt native folds.

The transient absorption data suggest that Fe^{II}-cyt c_{556} and Fe^{II}-cyt c-b_{562} refolding rates are faster than $10^4\ s^{-1}$. UV-visible spectra provide information about the immediate environment of the heme cofactor but do not directly report on the conformation of the polypeptide. To gain more insight into the submillisecond Fe^{II}-cyt c_{556} and Fe^{II}-cyt c-b_{562} folding dynamics, we repeated the photoinitiated refolding experiments in the presence of CO. The deeply buried iron centers of native c-b_{562} and c_{556} are six-coordinate and therefore not available for CO binding. Under denaturing conditions, the ferroheme remains low-spin, likely due to Met ligation in the sixth coordination site. Nevertheless, CO will replace Met as an Fe^{II} ligand in denatured c-b_{562} and c_{556}. We have examined the kinetics of CO rebinding to the heme after photodissociation from denatured Fe^{II}(CO)cyt c-b_{562} ([GuHCl] = 7 M) and Fe^{II}(CO)cyt c_{556} ([GuHCl] = 4 M). Under 1 atm (1 atm = 101.3 kPa) of CO, the rate constant for CO rebinding to the Fe^{II} heme is $\approx 65\ s^{-1}$. We have used CO ligation to the heme as a probe of the extent of heme protection afforded by the polypeptide during electron transfer-triggered refolding. If the polypeptide wraps around the heme rapidly ($>10^2\ s^{-1}$), little CO should bind to the heme. On the other hand, if folding is slower than $\approx 10^2\ s^{-1}$, substantial CO binding is expected. We find that at 7 M GuHCl, where formation of native, reduced c-b_{562} is disfavored, there is a major change in absorbance consistent with CO binding after reduction of the Fe^{III} protein. In contrast, very little CO binding is apparent under conditions favoring formation of the folded Fe^{II}-protein (4 M GuHCl) (Fig. 4).

Our electron transfer-triggered experiments reveal that early events ($t < 100\ \mu s$) in Fe^{II}-cyt c_{556} and Fe^{II}-cyt c-b_{562} refolding involve formation of a low-spin heme and some degree of heme encapsulation by the polypeptide. A lower limit to the time required for the heme to ligate a Met residue can be estimated from studies of tertiary contact dynamics in unfolded proteins and peptides (31–33). Met ligation to the heme in Fe^{II}-cyt c_{556} will produce polypeptide loops comprised of 96, 97, and 104 residues, and loop sizes of 39 and 90 residues in Fe^{II}-cyt c-b_{562} are possible. Energy-transfer quenching studies in synthetic polypeptides suggest that tertiary contact rate constants (k_c) for 90- to 100-residue loops are 10^6 to $10^7\ s^{-1}$ (32). These values compare with our observed rates of 10^5 to $10^6\ s^{-1}$ for formation of native heme absorption spectra in electron transfer-triggered Fe^{II}-cyt c_{556} and Fe^{II}-cyt c-b_{562} refolding experiments. The variation of these rate constants with [GuHCl] concentration is likely due in part to the viscosity dependence of the intrachain

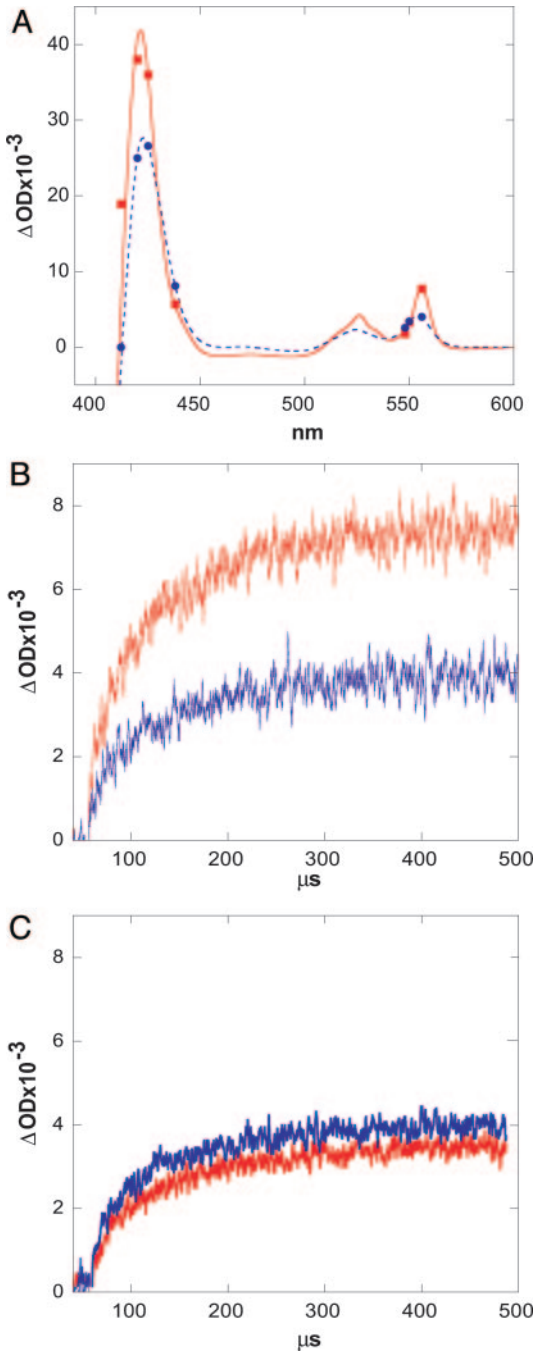

Fig. 3. ET-triggered refolding of Fe^{II}-cyt c-b_{562}. (*A*) Steady-state difference spectra between folded Fe^{II} and unfolded Fe^{III} (red) and between unfolded Fe^{II} and unfolded Fe^{III} (blue) c-b_{562}. Symbols indicate transient absorption changes measured 300 μs after 355-nm pulsed-laser excitation of NADH in the presence of denatured Fe^{III}-cyt c-b_{562} (red squares, [GuHCl] = 4 M; blue circles, [GuHCl] = 7 M). (*B*) Transient absorption kinetics observed at 556 nm upon reduction with NADH of c-b_{562} at 4 M GuHCl (red) and at 7 M GuHCl (blue). (*C*) Transient absorption kinetics observed at 548 nm.

diffusion dynamics that lead to tertiary contacts. In synthetic peptides, the logarithms of tertiary contact rates exhibit a linear dependence on [GuHCl] with m_c values $\{m_c = -RT\partial(\ln(k_c))/\partial[\text{GuHCl}] \sim 0.5\ (\text{kJ/mol})/\text{M}\}$ (34) that are substantially smaller than the m_k values $\{m_k = -RT\partial(\ln(k_{obs}))/\partial[\text{GuHCl}]\}$ found for the early kinetics phases of Fe^{II}-cyt c_{556} [$\approx$2.5 (kJ/mol)/M] and Fe^{II}-cyt c-b_{562} [$\approx$2.1 (kJ/mol)/M] refolding (Fig. 5). Fast-folding

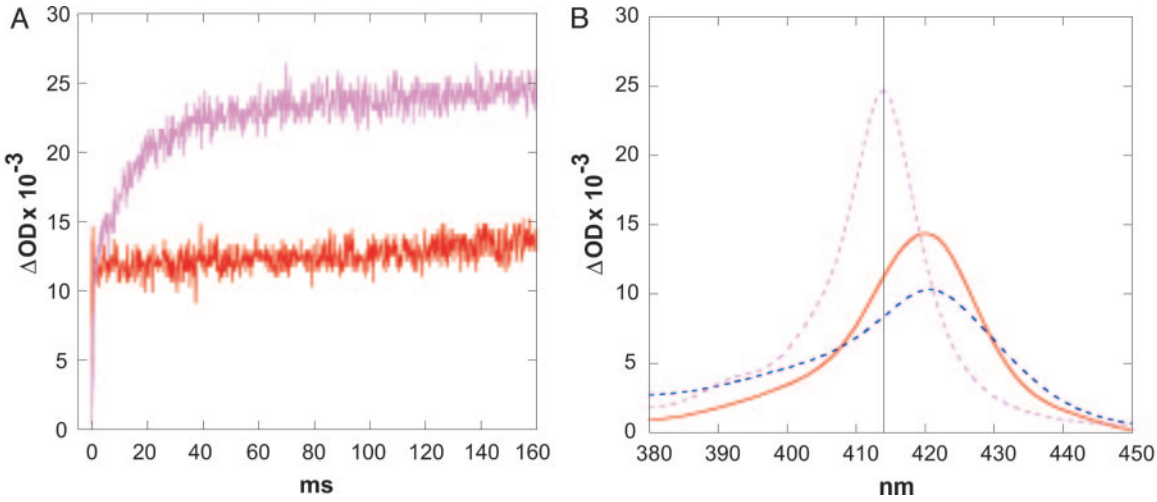

Fig. 4. ET-triggered refolding of Fe^{II}-cyt *c*-b_{562} in the presence of CO. (*A*) Transient absorption kinetics observed at 415 nm upon photochemical reduction (NADH) of *c*-b_{562} at 4 M GuHCl (red) and at 7 M GuHCl (pink) (1 atm CO). (*B*) Difference spectra between folded Fe^{II} and unfolded Fe^{III} (red), between unfolded Fe^{II} and unfolded Fe^{III} (blue), and between CO-Fe^{II} and unfolded Fe^{III} *c*-b_{562} (pink).

small proteins have been reported to have m_k values of 1–2 (kJ/mol)/M (34). The m_k values for larger proteins displaying two-state refolding kinetics are larger, 5–10 (kJ/mol)/M (34). These denaturant dependences observed for Fe^{II}-cyt c_{556} and Fe^{II}-cyt *c*-b_{562} refolding suggest that the early kinetics phases involve more than intrachain diffusion leading to Met-Fe ligation. Rapid Met-Fe ligation could facilitate refolding of Fe^{II}-cyt c_{556} and Fe^{II}-cyt *c*-b_{562}, because formation of one or more strong native tertiary contacts will substantially reduce the size of the conformational space available to the polypeptide (35). Constraining the folding energy landscape in this manner could lead to a substantial reduction in the time required to find the native structure (36).

After reduction of the unfolded oxidized proteins, CO will bind to the ferroheme under solution conditions where formation of native structure is disfavored. The observed rate constant for CO binding to denatured Fe^{II}-cyt c_{556} and Fe^{II}-cyt *c*-b_{562} (65 s^{-1}) is ≈10 times smaller than the corresponding rate found for Fe^{II}-cyt *c*′ (10), and ≈20 times smaller than the rate for Fe^{II}-cyt *c* (37). The smaller CO binding rate constant for Fe^{II}-cyt c_{556} and Fe^{II}-cyt *c*-b_{562} may be a consequence of stronger Met binding to the reduced denatured proteins. Indeed, the similarity in the absorption spectra of folded and denatured reduced proteins (Fig. 2) suggests that Met is completely bound in the denatured forms. The Soret absorption of denatured Fe^{II}-cyt *c*′ is less intense than that of denatured Fe^{II}-cyt c_{556} and Fe^{II}-cyt *c*-b_{562}, possibly because of less complete Met binding.

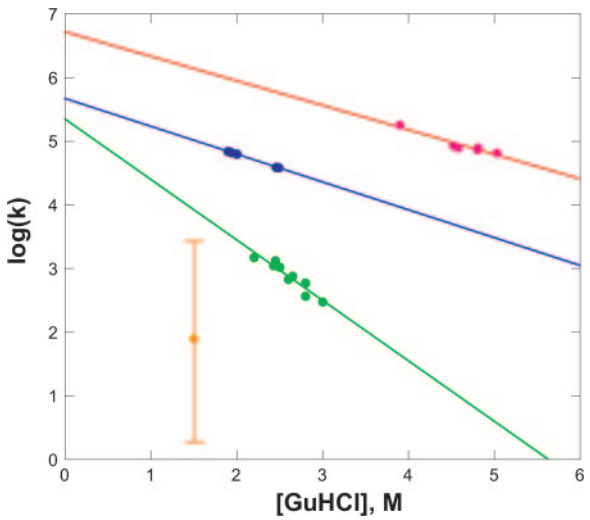

Fig. 5. Folding rates as a function of [GuHCl]. Red, Fe^{II}-cyt *c*-b_{562}; blue, Fe^{II}-cyt c_{556}; green, Fe^{II}-cyt b_{562} (11); yellow, Fe^{II}-cyt *c*′ (the vertical bar reflects the range of observed rate constants) (10).

Our finding that CO does not bind to the Fe^{II}-cyt c_{556} and Fe^{II}-cyt *c*-b_{562} hemes under GuHCl conditions favoring folding points to encapsulation of the heme by the polypeptide in <10 ms. The spectroscopic data do not reveal whether the polypeptide has developed secondary and tertiary structure by this time. Ultrafast mixing measurements on a F65W mutant of apo-cyt b_{562}, which adopts a three-helix-bundle fold (19, 38), are consistent with a refolding rate constant of 2,600 s^{-1} in the absence of denaturant (12). This value represents a reasonable upper limit to the folding rate for the holoprotein and is in line with the lower limit indicated by our CO ligation measurements.

The refolding of Fe^{II}-cyt c_{556} and Fe^{II}-cyt *c*-b_{562} clearly begins from an extensively denatured state. This finding contrasts with recent results on Fe^{II}-cyt b_{562} (12) where, as we had suggested earlier (11), heme dissociation preselects fast-folding members of the denatured ensemble. The only events revealed by changes in heme absorption spectra in Fe^{II}-cyt c_{556} and Fe^{II}-cyt *c*-b_{562} occur on very early time scales (1–10 μs) and involve Met-Fe ligation processes. The absence of separate kinetics phases attributable to heme encapsulation by the polypeptide, and the observation that the heme is protected from CO binding, confirm that a substantial degree of refolding occurs on submillisecond time scales. This behavior contrasts sharply with results from Fe^{II}-cyt *c*′ experiments in which changes in heme spectra were observed on time scales from 10^{-4} s to 10^{1} s after reduction of the unfolded oxidized protein. We suggest that formation of one persistent native contact in the early stages of Fe^{II}-cyt c_{556} and Fe^{II}-cyt *c*-b_{562} refolding puts each polypeptide on a fast track to its native structure (36). The slower and more complex refolding kinetics found for Fe^{II}-cyt *c*′ may be a consequence of weaker S(Met)-Fe bonding in the denatured protein.

This research was supported by National Institutes of Health Grant GM068461, Department of Energy Grant DE-FG02-02ER15359, and the Arnold and Mabel Beckman Foundation.

1. Plaxco, K. W., Larson, S., Ruczinski, I., Riddle, D. S., Thayer, E. C., Buchwitz, B., Davidson, A. R. & Baker, D. (2000) *J. Mol. Biol.* **298,** 303–312.
2. Wolynes, P. G. (1996) *Proc. Natl. Acad. Sci. USA* **93,** 14249–14255.
3. Ivankov, D. N., Garbuzynskiy, S. O., Alm, E., Plaxco, K. W., Baker, D. & Finkelstein, A. V. (2003) *Protein Sci.* **12,** 2057–2062.
4. Zhou, Y. & Karplus, M. (1999) *Nature* **401,** 400–403.
5. Ferguson, N., Capaldi, A. P., James, R., Kleanthous, C. & Radford, S. E. (1999) *J. Mol. Biol.* **286,** 1597–1608.
6. Kragelund, B. B., Osmark, P., Neergaard, T. B., Schiødt, J., Kristiansen, K., Knudsen, J., Poulsen, F. M. (1999) *Nat. Struct. Biol.* **6,** 594–601.
7. Teilum, K., Kragelund, B. B., Knudsen, J. & Poulsen, F. (2000) *J. Mol. Biol.* **301,** 1307–1314.
8. Thomsen, J. K., Kragelund, B. B., Teilum, K., Knudsen, J. & Poulsen, F. M. (2002) *J. Mol. Biol.* **318,** 805–814.
9. Lee, J. C., Engman, K. C., Tezcan, F. A., Gray, H. B. & Winkler, J. R. (2002) *Proc. Natl. Acad. Sci. USA* **99,** 14778–14782.
10. Lee, J. C., Gray, H. B. & Winkler, J. R. (2001) *Proc. Natl. Acad. Sci. USA* **98,** 7760–7764.
11. Wittung-Stafshede, P., Lee, J. C., Winkler, J. R. & Gray, H. B. (1999) *Proc. Natl. Acad. Sci. USA* **96,** 6587–6590.
12. Garcia, P., Bruix, M., Rico, M., Ciofi-Baffoni, S., Banci, L., Shastry, M. C. R., Roder, H., Woodyear, T. d. L., Johnson, C. M., Fersht, A. R. & Barker, P. D. (2005) *J. Mol. Biol.* **346,** 331–344.
13. Moore, G. R. & Pettigrew, G. W. (1990) *Cytochromes c: Evolutionary, Structural, and Physicochemical Aspects* (Springer, New York).
14. Scott, R. A. & Mauk, A. G. (1996) (University Science Books, Sausalito, CA), pp. 738.
15. Allen, J. W. A., Barker, P. D. & Ferguson, S. J. (2003) *J. Biol. Chem.* **278,** 52075–52083.
16. McGuirl, M. A., Lee, J. C., Lyubovitsky, J. G., Thanyakoop, C., Richards, J. H., Gray, H. B. & Winkler, J. R. (2003) *Biochim. Biophys. Acta* **1619,** 23–28.
17. Lederer, F., Glatigny, A., Bethge, P. H., Bellamy, H. D. & Mathews, F. S. (1981) *J. Mol. Biol.* **148,** 427–448.
18. Bertini, I., Faraone-Mennella, J., Gray, H. B., Luchinat, C., Parigi, G. & Winkler, J. R. (2004) *J. Biol. Inorg. Chem.* **9,** 224–230.
19. Arnesano, F., Banci, L., Bertini, I., Faraone-Mennella, J., Rosato, A., Barker, P. D. & Fersht, A. R. (1999) *Biochemistry* **38,** 8657–8670.
20. Shibata, N., Iba, S., Misaki, S., Meyer, T. E., Bartsch, R. G., Cusanovich, M. A., Morimoto, Y., Higuchi, Y. & Yasuoka, N. (1998) *J. Mol. Biol.* **284,** 751–760.
21. Khandke, K. M., Fairwell, T., Chait, B. T. & Manjula, B. N. (1989) *Int. J. Pept. Protein Res.* **34,** 118–123.
22. Arslan, E., Schulz, H., Zufferey, R., Kunzler, P. & Thony-Meyer, L. (1998) *Biochem. Biophys. Res. Commun.* **251,** 744–747.
23. Moore, G. R., Williams, R. J. P., Peterson, J., Thomson, A. J. & Mathews, F. S. (1985) *Biochim. Biophys. Acta* **829,** 83–96.
24. Itagaki, E. & Hager, L. P. (1966) *J. Biol. Chem.* **241,** 3687–3695.
25. Stowell, M. H. B., Larsen, R. W., Winkler, J. R., Rees, D. C. & Chan, S. I. (1993) *J. Phys. Chem.* **97,** 3054–3057.
26. Nozaki, Y. (1972) *Methods Enzymol.* **26,** 43–50.
27. Pascher, T., Chesick, J. P., Winkler, J. R. & Gray, H. B. (1996) *Science* **271,** 1558–1560.
28. Telford, J. R., Wittung-Stafshede, P., Gray, H. B. & Winkler, J. R. (1998) *Acc. Chem. Res.* **31,** 755–763.
29. Telford, J. R., Tezcan, F. A., Gray, H. B. & Winkler, J. R. (1999) *Biochemistry* **38,** 1944–1949.
30. Orii, Y. (1993) *Biochemistry* **32,** 11910–11914.
31. Bieri, O., Wirz, J., Hellrung, B., Schutkowski, M., Drewello, M. & Kiefhaber, T. (1999) *Proc. Natl. Acad. Sci. USA* **96,** 9597–9601.
32. Krieger, F., Fierz, B., Bieri, O., Drewello, M. & Kiefhaber, T. (2003) *J. Mol. Biol.* **332,** 265–274.
33. Chang, I.-J., Lee, J. C., Winkler, J. R. & Gray, H. B. (2003) *Proc. Natl. Acad. Sci. USA* **100,** 3838–3840.
34. Möglich, A., Krieger, F. & Kiefhaber, T. (2005) *J. Mol. Biol.* **345,** 153–162.
35. Dyer, R. B., Maness, S. J., Peterson, E. S., Franzen, S., Fesinmeyer, R. M. & Andersen, N. (2004) *Biochemistry* **43,** 11560–11566.
36. Ittah, V. & Haas, E. (1995) *Biochemistry* **34,** 4493–4506.
37. Arcovito, A., Gianni, S., Brunori, M., Travaglini-Allocatelli, C. & Bellelli, A. (2001) *J. Mol. Biol.* **276,** 41073–41078.
38. Laidig, K. E. & Daggett, V. (1996) *Folding Des.* **1,** 335–346.